



CHORUS

This is the accepted manuscript made available via CHORUS. The article has been published as:

High Conductance 2D Transport around the Hall Mobility Peak in Electrolyte-Gated Rubrene Crystals

Wei Xie, Shun Wang, Xin Zhang, C. Leighton, and C. Daniel Frisbie

Phys. Rev. Lett. **113**, 246602 — Published 10 December 2014

DOI: [10.1103/PhysRevLett.113.246602](https://doi.org/10.1103/PhysRevLett.113.246602)

High Conductance 2D Transport around the Hall Mobility Peak in Electrolyte-Gated Rubrene Crystals

Wei Xie¹, Shun Wang^{1,}, Xin Zhang¹, C. Leighton¹ and C. Daniel Frisbie¹*

¹Department of Chemical Engineering and Materials Science, University of Minnesota, Minneapolis, Minnesota, 55455, USA

*Current Address: Department of Physics and Astronomy, Key Laboratory of Artificial Structures and Quantum Control (Ministry of Education), Shanghai Jiao Tong University, Shanghai, 200240, China

PACS numbers: 72.80.Le, 81.05.Fb, 72.20.My, 72.20.Dp

Abstract

We report the observation of the Hall effect at hole densities up to $6 \times 10^{13} \text{ cm}^{-2}$ (0.3 holes/molecule) on the surface of electrolyte-gated rubrene crystals. The perplexing peak in conductance as a function of gate voltage is confirmed to result from a maximum in mobility, which reaches $4 \text{ cm}^2\text{V}^{-1}\text{s}^{-1}$ at $2.5 \times 10^{13} \text{ cm}^{-2}$. Measurements to liquid helium temperatures reveal that this peak is markedly asymmetric, band-like and hopping-type transport occurring on the low density side, while unconventional, likely electrostatic-disorder-affected transport dominates the high density side. Most significantly, near the mobility peak the temperature coefficient of resistance remains positive to as low as 120 K, the low temperature resistance becomes weakly temperature dependent, and the conductance reaches within a factor of 2 of e^2/h , revealing conduction unprecedentedly close to a two dimensional (2D) metallic state.

Tuning transitions among electronic ground states (*e.g.*, semiconducting, metallic, superconducting) in molecular crystals is an active research area [1]. Of the techniques to control carrier density in such systems, chemical doping has perhaps facilitated most advances, including superconductivity in alkali-metal-doped C₆₀ [2] and linear hydrocarbons such as picene [3]. Solid-state charge transfer between an electron acceptor and donor to form charge-transfer complexes has also been successful, the quasi-one-dimensional metal TTF-TCNQ [4] and the superconductor (TMTSF)₂PF₆ [5] being good examples. Electrostatic gating in the field-effect transistor (FET) geometry is an attractive complementary approach, enabling reversible fine-tuning of carrier density, in a single sample, while minimizing structural/chemical disorder [6]. An important recent breakthrough in this direction is the observation of band-like transport [7] on the surface of electrostatically-gated crystals such as rubrene, as evidenced by thermal disorder-limited conduction [8–10], and equivalence of Hall and FET mobilities [11]. This was restricted to high temperatures though (close to 300 K), and to a vacuum-gap architecture with the crystal surface unperturbed by dielectric-induced disorder [12]. Due to the modest hole densities achieved ($\sim 10^{10} \text{ cm}^{-2}$) the sheet resistances remain high (M Ω range [9]), despite mobilities $\mu > 10 \text{ cm}^2\text{V}^{-1}\text{s}^{-1}$. Such resistances significantly exceed the two-dimensional (2D) quantum value ($h/e^2 \approx 25.8 \text{ k}\Omega$) [13], meaning that a wide potential regime of transport remains unexplored at molecular semiconductor surfaces. Probing high charge density 2D transport at the surface of rubrene is thus of great interest, *provided* relatively high mobilities can be preserved.

In *inorganic* 2D semiconductor systems, such as Si metal-oxide-semiconductor FETs (MOSFETs) and GaAs-based heterostructures, a startling observation enabled by attainment of carrier densities $\sim 10^{11} \text{ cm}^{-2}$, while maintaining high mobility, was the 2D metallic state

previously thought forbidden [14,15]. While the origin of this state remains unclear, electron-electron (e-e) interactions are considered critical [15]. Although mobilities in molecular semiconductors remain far lower than Si and GaAs, hindering attainment of conductances $\sim e^2/h$ at low densities (where e-e interactions are strongest), factors such as low dielectric constants and high effective masses do favor strong correlations. There is thus strong motivation to probe high density, high mobility transport at rubrene surfaces, as the ultimate limits on 2D molecular semiconductor conductance, which could conceivably involve a metallic state, remain unclear.

In this work, we use electrolyte gating [16,17] in the electric double layer transistor (EDLT) geometry to probe transport at the surface of rubrene crystals at hole densities, p , up to $6 \times 10^{13} \text{ cm}^{-2}$, *i.e.*, 0.32 holes per molecule, three orders of magnitude larger than in vacuum-gap devices. The conductance is found to *decrease* at the highest p , a phenomenon emerging as common in organic EDLTs but incompletely understood [18–20]. Hall effect measurements across this conductance peak (the first of their kind) establish that it is in fact a maximum in mobility at $\mu_{\text{Hall}} = 4 \text{ cm}^2\text{V}^{-1}\text{s}^{-1}$, $p = 2.5 \times 10^{13} \text{ cm}^{-2}$, band-like transport [7,21] being retained despite the large p . Cryogenic resistance-temperature (R - T) measurements down to 8 K reveal that the transport is asymmetric across this peak, being conventional at low p but suggestive of electrostatic-disorder at high p . Most significantly, around the peak conductance we obtain weak $R(T)$, positive dR/dT over a substantial T range, and minimum R of 50-60 k Ω , within a factor of 2 of h/e^2 . We thus significantly extend the regime of probed conductance at the surface of rubrene crystals, demonstrating transport remarkably close to a 2D metal.

Rubrene EDLTs were constructed on poly-dimethylsiloxane (PDMS) stamps by first fabricating vacuum-gap transistors [22], using a bottom-contact Hall-bar geometry as shown in **Figs. 1(a),(b)** (see Section 1 in Supplemental Material for further details [23]). The ionic liquid (IL), [1-butyl-1-methylpyrrolidinium] [tris(pentafluoroethyl)trifluorophosphate] ([P14][FAP], **Fig. 1(a)**) was then introduced into the gap *via* capillarity-assisted filling. Different ILs have been used to accumulate carrier densities up to 10^{14} cm⁻² in a variety of semiconductors [24,25]. This specific IL was employed here because it yields EDLTs with high mobility and large gate voltage (V_G) window, as shown previously [26]. The latter is important since the electrochemical window of ILs can limit the maximum V_G [16]. Both the IL composition and the temperature range to operate the device have been optimized to achieve large hole densities [26]. *p*-dependent measurements were made by applying V_G at 240 K (and measuring transfer curves), then cooling to < 220 K where the IL froze. *T*-dependent four-terminal sheet resistance (DC) and Hall measurements (AC, 13.7 Hz) were then performed, with careful checks for non-Ohmicity. Notably, measurements were possible down to 8 K, limited only by contact resistance. Such cryogenic measurements are challenging with vacuum-gap devices [9,27], and we deduce that ILs in the gate-crystal gap mechanically stabilize the devices with respect to thermal expansion mismatch, an important advance.

The transfer characteristic of a typical rubrene EDLT (Device #1) at 240 K is shown in **Fig. 1(c)**. The device turns on at $V_G = 1.1$ V, has an ON/OFF ratio $> 10^3$, and displays gate leakage current much smaller than the drain current, I_D . Clearly, $I_D(V_G)$ exhibits a pronounced, reversible peak. As discussed above, conductance peaks of this type are emerging as common in electrolyte-gated organic crystals and polymers [26,28,29], although they are incompletely

understood [18,20]. Importantly, **Fig. 1(d)** suggests that the peak arises from a maximum in μ . In this figure the μ values shown are calculated as $\mu_{\text{gate}} = 1/(p_{\text{gate}}eR)$, where p_{gate} is the hole density extracted from the gate displacement current, as in Ref [26]. p_{gate} increases linearly with increasing $|V_G|$, reaching $3 \times 10^{13} \text{ cm}^{-2}$ at -1.0 V. Due to the peak in $I_D(V_G)$ (Fig. 1(c)), a peak in μ_{gate} occurs near -0.25 V (Fig. 1(d)). Note that the maximum μ_{gate} exceeds $4 \text{ cm}^2\text{V}^{-1}\text{s}^{-1}$ at 240 K, a decrease from vacuum-gap devices of only a factor of $3 \sim 5$, despite the three orders of magnitude increase in p .

To probe whether the transport remains band-like [7], and to directly confirm the maximum in $\mu(V_G)$, we performed V_G -dependent Hall measurements. **Fig. 2(a)** shows the time evolution of the Hall voltage (V_{Hall} , black points) in Device #1 in response to a time-varying applied magnetic field ($\mu_0 H$, solid line), at $V_G = -0.5 \text{ V}$ and $T = 200 \text{ K}$. A clear Hall signal is observed with negligible drift; similarly robust Hall effect is obtained over the entire operational window, from $V_G = 0.3 \text{ V}$ to -1.0 V . In **Fig. 2(b)** these results are presented in more familiar form by plotting the $H = 0$ background-subtracted Hall resistance, R_{Hall} , vs. $\mu_0 H$, at V_G 's of 0.2 V and -0.75 V , *i.e.*, straddling the conductance peak (Fig. 1(c)). We find R_{Hall} to be linear with H , with a positive Hall coefficient consistent with holes. The significant magnitude of the Hall effect, and the correspondence with the expected carrier type, are consistent with band-like transport [7,21], as opposed to hopping [30,31].

More quantitative verification of band-like transport is enabled by **Fig. 2(c)**, where the V_G dependence of the hole densities measured from gate displacement current (p_{gate}) and Hall effect (p_{Hall}) are compared. Out to -0.5 V , Hall and FET measurements agree closely, consistent with

band-like transport at this T (200 K). Although prior work on rubrene EDLTs probed p via displacement current and capacitance [17,26], Fig. 2(c) provides the first direct Hall-effect-based confirmation of free hole densities $\sim 10^{13}$ cm $^{-2}$. Reassuringly, a linear fit to $p_{\text{Hall}}(V_G)$ in this range gives a specific capacitance ≈ 2.5 $\mu\text{F}/\text{cm}^2$, in accord with the double layer capacitance [19,26]. For V_G 's more negative than -0.5 V, however, Hall and FET measurements disagree, p_{Hall} becoming progressively larger than p_{Gate} . Generally this could indicate a diminishing Hall coefficient [32] due to the onset of a crossover from band-like to hopping transport, but we demonstrate below that the situation here may be more complex. In any case, **Fig. 2(d)** shows that the Hall data indeed confirm the mobility peak suggested by Fig. 1(d), an important finding. In fact, $\mu_{\text{Hall}}(p_{\text{Hall}})$ plots for five devices studied are quantitatively similar, with peak μ_{Hall} between 3.1 and 4.1 cm $^2\text{V}^{-1}\text{s}^{-1}$, occurring at p_{Hall} from 2.0×10^{13} to 2.6×10^{13} cm $^{-2}$ (Fig. S1, Supplemental Material [23]). This Hall mobility peak further confirms, at least in our devices, that the widely-observed I_D peak is not due to V_G -dependent contact resistance [33]. We also note that we clearly observe a *peak* in μ and I_D rather than the I_D *saturation* shown in Ta $_2$ O $_5$ -gated rubrene transistors by Fratini *et al* [34], at somewhat lower p and μ . **Fig. 2(e)** shows that, as anticipated from Fig. 1(c), the 200 K R values reach a minimum at -0.5 V, before exhibiting an upturn at more negative V_G 's. R falls as low as 60 k Ω at this T , within a factor of 2 of h/e^2 .

In order to more deeply probe the nature of the mobility peak, the issue of band-like *vs.* hopping transport, and the high conductance at the peak, T -dependent measurements were made (Fig. 3). To illustrate these, we first show (**Fig. 3(a)**) a representative $\mu_{\text{Hall}} - p_{\text{Hall}}$ relation (from Device #2), with each of the measured p_{Hall} values labeled *a* to *h*. These span from $p_{\text{Hall}} = 1.0 \times 10^{13}$ to 6.0×10^{13} cm $^{-2}$ (conversion to holes/molecule is shown on the top axis), encompassing

the peak. The three insets to Fig. 3(a) show $\mu_{\text{Hall}}(T)$ at points c , e , and g , *i.e.*, before, at, and beyond the peak. At point c , μ decreases slowly on cooling, from $2.5 \text{ cm}^2\text{V}^{-1}\text{s}^{-1}$ at 200 K to $0.4 \text{ cm}^2\text{V}^{-1}\text{s}^{-1}$ at 60 K, and Arrhenius fits result in an activation energy of only 14 meV. Although the 200 K transport is band-like at this p (based on equivalence of Hall and FET mobilities (Fig. 2(c)), and the absolute magnitude of $2.5 \text{ cm}^2\text{V}^{-1}\text{s}^{-1}$), the decrease to only $0.4 \text{ cm}^2\text{V}^{-1}\text{s}^{-1}$ at low T suggests a possible crossover to hopping, as confirmed below. At hole densities such as point e on the other hand (near the peak), where band-like transport is again implicated by Fig. 2(c) and the absolute mobility magnitude ($3.6 \text{ cm}^2\text{V}^{-1}\text{s}^{-1}$), μ_{Hall} instead remains constant at 3 - 4 $\text{cm}^2\text{V}^{-1}\text{s}^{-1}$ upon cooling, indicating that band-like transport is preserved to lower T . At point g however, which is beyond the peak but has 200 K mobility similar to c , μ_{Hall} falls rapidly on cooling, the activation energy (48 meV) being $3\times$ larger than at c . The *asymmetry* of the mobility peak is thus apparent not only from the shape of $\mu_{\text{Hall}}(p_{\text{Hall}})$ (Fig. 3(a), main panel), but also from $\mu_{\text{Hall}}(T)$ around the peak (Fig. 3(a) insets).

This asymmetry is further highlighted in **Fig. 3(b)** where $R(T)$ is plotted on a log-linear scale at points $a-h$. As shown in the left panel, $R(T)$ evolves from a monotonic increase on cooling at point a (clearly insulating), to a situation at c where R first decreases down to 190 K, before increasing at lower T . This continues at d and e (middle panel), dR/dT remaining positive to lower T as p increases. At point e (near the mobility peak) we obtain positive dR/dT to as low as 120 K, a minimum R under 60 k Ω , and an increase on cooling to the lowest T of only a factor of six. The positive dR/dT at high- T from $b-e$ clearly indicates a contribution from thermal disorder, [8] further evidence that band-like transport is maintained in this region, despite the large p . Going beyond this, to point f , results in little change in high- T resistance, but a rapid

increase at low T . Eventually, at g and h (right panel) we obtain low, weakly T -dependent R at high T , but with remarkably rapid increases below 100-150 K, *i.e.*, reentrance of a strong insulator.

The left and right panels of Fig. 3(b) suggest different functional forms for $R(T)$ before and after the mobility peak. This is borne out by Fig. 4, where $R(T)$ at points a - f (*i.e.*, up to and slightly beyond the peak) are plotted as $\log_{10}R$ vs. T^{-1} (**Fig. 4(a)**), while $R(T)$ at points g and h (beyond the peak) are plotted as $\log_{10}R$ vs. $\log_{10}T$ (**Fig. 4(b)**). At points a and b (Fig. 4(a)), simple activated behavior is observed over a wide range, *i.e.*, $R = R_0 \exp(T_0/T)^n$, with $n = 1$, R_0 a prefactor, and E_A the activation energy. This continues at c and d , albeit with increasing deviations from linearity at low T . Logarithmic derivative analysis [35,36] (see Fig. S2 in Supplemental Material [23]), illustrates that this is due to a transition from simple activation ($n = 1$) at higher T to Efros-Shklovskii variable range hopping [37] (VRH, $n = 1/2$) at lower T , as is common in semiconductors, including organics [38]. Magnetoresistance was also measured at c , the analysis of which (see Fig. S3, Supplemental Material [23]) further confirms VRH. This situation changes at point e however (near the mobility peak), where $R(T)$ becomes so weak (Fig. 4(a)) that logarithmic derivative analysis reveals no regime of any exponential T dependence (Fig. S2 in [23]). Continuing to f , and eventually g and h (Fig. 4(b), beyond the mobility peak) the form of $R(T)$ again changes. As illustrated in Fig. 4(b), and confirmed by the logarithmic derivative (Fig. S2 in [23]), $R(T)$ in fact follows a power-law over a considerable range, *i.e.*, $R = R_{00}T^{-m}$ with R_{00} a pre-factor, and m an exponent that increases from 4.0 at g to 7.0 at h . This is clearly different to low p , and represents an unusual observation, multi-phonon hopping in certain specific situations [39,40] being the only mechanism we are aware of following this form.

Further insight is provided by the inset to Fig. 4(a), where E_A is plotted vs. p_{Hall} , showing a rapid decrease from points a to d . At point e (near the peak), as already emphasized, $R(T)$ becomes weakly T -dependent, a force-fit to an activated form at low T yielding E_A of only 1.1 meV, essentially identical to $k_B T$ at the lowest T (dashed line in the inset to Fig. 4(a)). The transport is thus so weakly insulating that an exponential fit in this T range is not meaningful. Further increase in p to points f - h results in a rapid increase in E_A from a force-fit to an Arrhenius form (Fig. 4(b)), again highlighting the reentrant strongly insulating state. As a final comment on the weak T dependence at point e , note that $R(T)$ also does not adhere to $\ln(T)$, meaning that a crossover to 2D weak localization is not apparent. Similarly, while the conductance (G) vs. T at point e does not yet suggest an obviously finite $T = 0$ value, the extrapolated G is remarkably close to the origin (Fig. 4(b), inset), again highlighting the proximity to a metallic state. $G(T)$ at d and f are shown for comparison, and are clearly insulating.

Two main issues warrant further discussion: the prospect of a 2D metal on the surface of rubrene, and the origin of the mobility peak. Regarding the former, we first summarize that at the peak mobility in our EDLTs we have demonstrated band-like transport to at least as low as 70 K, positive dR/dT to 120 K, non-exponential $R(T)$ to 8 K, R within a factor of 2 of h/e^2 , and close to finite G ($T \rightarrow 0$). As already mentioned, in inorganics e-e interactions are thought essential for 2D metallicity. The parameter r_s , simply the ratio of the e-e interaction (E_{e-e}) to Fermi energies (E_F) has proven useful for quantifying these electronic correlations [14]. Using $E_{e-e} =$

$$\frac{e^2}{4\pi\epsilon_r\epsilon_0}(\pi p)^{1/2} \text{ and } E_F = \frac{\pi\hbar^2 p}{2m_h^*}, \text{ where } \epsilon_r \text{ and } \epsilon_0 \text{ are relative and vacuum permittivities and } m_h^* \text{ is}$$

the hole mass, we estimate $r_s \approx 10$ for our rubrene EDLTs at $p = 2.5 \times 10^{13} \text{ cm}^{-2}$. This is

significant, as 2D metallic states emerge in inorganic semiconductors at $r_s \sim 10$, considered a threshold for strongly correlated electronic liquids [11]. This not only rationalizes the $G \sim e^2/h$ we observe here, but suggests an insulator-metal transition on the surface of rubrene could be within reach with EDLT improvements. Turning to the mobility peak, note that explanations based both on the structure of the organic conductor valence band [41], Coulombic interactions between holes [34], and Coulombic interactions between holes and the EDL have been discussed. The latter has been analyzed in detail recently [18,20], suggesting that the non-uniform potential from the EDL leads to V_G -dependent hole-trapping. We propose that this provides qualitative rationalization for our observations, the suppressed μ and anomalous $R(T)$ at the highest p 's resulting from inhomogeneous percolative 2D semiconducting transport due to EDL-induced electrostatic disorder [42]. This could potentially be alleviated by smoothing the disorder potential, perhaps by simply increasing the size of the IL ions; this could improve μ at the expense of p , a strategy that could also help to realize the aforementioned 2D metallic state.

In summary, we have explored transport on the surface of electrolyte-gated rubrene crystals at charge densities up to 0.3 holes/molecule *via* T -dependent resistance and Hall measurements. As a function of p the transport first evolves in a conventional manner from strongly insulating to conductive, then to a reentrant strongly insulating state ascribed to gate-induced electrostatic disorder. Around the peak mobility, where band-like transport is maintained despite the large p , all measurements and analyses point to a state remarkably close to a strongly correlated 2D metal, which may well lie within reach with further innovations in EDLTs.

Acknowledgements: This work was supported by the MRSEC program of the NSF under the award number DMR-0819885 and the Department of Energy, Basic Energy Sciences under DESC 0004200. W.X also acknowledges the University of Minnesota for a Doctoral Dissertation Fellowship. We acknowledge useful discussions with Prof. B. Shklovskii.

References

- [1] E. Silinsh and V. Capek, *Organic Molecular Crystals: Interaction, Localization, and Transport Phenomena* (American Institute of Physics, 1994).
- [2] R. C. Haddon, *Acc. Chem. Res.* **25**, 127 (1992).
- [3] R. Mitsuhashi, Y. Suzuki, Y. Yamanari, H. Mitamura, T. Kambe, N. Ikeda, H. Okamoto, A. Fujiwara, M. Yamaji, N. Kawasaki, Y. Maniwa, and Y. Kubozono, *Nature* **464**, 76 (2010).
- [4] M. J. Cohen, L. B. Coleman, A. F. Garito, and A. J. Heeger, *Phys. Rev. B* **10**, 1298 (1974).
- [5] D. Jérôme, A. Mazaud, M. Ribault, and K. Bechgaard, *J. Phys. Lett.* **41**, 95 (1980).
- [6] C. H. Ahn, M. Di Ventura, J. N. Eckstein, C. D. Frisbie, M. E. Gershenson, A. M. Goldman, I. H. Inoue, J. Mannhart, A. J. Millis, A. F. Morpurgo, D. Natelson, and J.-M. Triscone, *Rev. Mod. Phys.* **78**, 1185 (2006).
- [7] A. Troisi, *Chem. Soc. Rev.* **40**, 2347 (2011).
- [8] A. Troisi and G. Orlandi, *Phys. Rev. Lett.* **96**, 086601 (2006).
- [9] V. Podzorov, E. Menard, A. Borissov, V. Kiryukhin, J. A. Rogers, and M. E. Gershenson, *Phys. Rev. Lett.* **93**, 086602 (2004).
- [10] W. Xie, K. A. McGarry, F. Liu, Y. Wu, P. P. Ruden, C. J. Douglas, and C. D. Frisbie, *J. Phys. Chem. C* **117**, 11522 (2013).
- [11] V. Podzorov, E. Menard, J. A. Rogers, and M. E. Gershenson, *Phys. Rev. Lett.* **95**, 226601 (2005).
- [12] I. N. Hulea, S. Fratini, H. Xie, C. L. Mulder, N. N. Iossad, G. Rastelli, S. Ciuchi, and A. F. Morpurgo, *Nat. Mater.* **5**, 982 (2006).
- [13] N. F. Mott, *Metal-Insulator Transitions* (Taylor & Francis, 1974).
- [14] E. Abrahams, S. V. Kravchenko, and M. P. Sarachik, *Rev. Mod. Phys.* **73**, 251 (2001).
- [15] E. Abrahams, *50 Years of Anderson Localization* (World Scientific, 2010).
- [16] S. H. Kim, K. Hong, W. Xie, K. H. Lee, S. Zhang, T. P. Lodge, and C. D. Frisbie, *Adv. Mater.* **25**, 1822 (2013).
- [17] W. Xie and C. D. Frisbie, *MRS Bull.* **38**, 43 (2013).
- [18] Y. Xia, W. Xie, P. P. Ruden, and C. D. Frisbie, *Phys. Rev. Lett.* **105**, 036802 (2010).
- [19] F. Liu, W. Xie, S. Shi, C. Daniel Frisbie, and P. Paul Ruden, *Appl. Phys. Lett.* **103**, 193304 (2013).
- [20] W. Xie, F. Liu, S. Shi, P. P. Ruden, and C. D. Frisbie, *Adv. Mater.* **26**, 2527 (2014).
- [21] J.-F. Chang, T. Sakanoue, Y. Olivier, T. Uemura, M.-B. Dufourg-Madec, S. G. Yeates, J. Cornil, J. Takeya, A. Troisi, and H. Sirringhaus, *Phys. Rev. Lett.* **107**, 066601 (2011).
- [22] Y. Xia, J. H. Cho, J. Lee, P. P. Ruden, and C. D. Frisbie, *Adv. Mater.* **21**, 2174 (2009).
- [23] See Supplemental Material at <http://> for reproducibility of mobility peak from Hall effect, extraction of exponents and powers in $R(T)$, and magnetoresistance, which includes Refs. [22, 35-37, 43]
- [24] K. Ueno, S. Nakamura, H. Shimotani, A. Ohtomo, N. Kimura, T. Nojima, H. Aoki, Y. Iwasa, and M. Kawasaki, *Nat. Mater.* **7**, 855 (2008).
- [25] J. Ye, M. F. Craciun, M. Koshino, S. Russo, S. Inoue, H. Yuan, H. Shimotani, A. F. Morpurgo, and Y. Iwasa, *Proc. Natl. Acad. Sci.* **108**, 13002 (2011).
- [26] W. Xie and C. D. Frisbie, *J. Phys. Chem. C* **115**, 14360 (2011).
- [27] H. Xie, H. Alves, and A. F. Morpurgo, *Phys. Rev. B* **80**, 245305 (2009).
- [28] M. J. Panzer and C. D. Frisbie, *J. Am. Chem. Soc.* **127**, 6960 (2005).
- [29] B. D. Paulsen and C. D. Frisbie, *J. Phys. Chem. C* **116**, 3132 (2012).
- [30] P. G. Le Comber, D. I. Jones, and W. E. Spear, *Philos. Mag.* **35**, 1173 (1977).

- [31] T. Uemura, M. Yamagishi, J. Soeda, Y. Takatsuki, Y. Okada, Y. Nakazawa, and J. Takeya, *Phys. Rev. B* **85**, (2012).
- [32] H. Tamura, M. Tsukada, H. Ishii, N. Kobayashi, and K. Hirose, *Phys. Rev. B* **87**, 155305 (2013).
- [33] H. Shimotani, H. Asanuma, and Y. Iwasa, *Jpn. J. Appl. Phys.* **46**, 3613 (2007).
- [34] S. Fratini, H. Xie, I. N. Hulea, S. Ciuchi, and A. F. Morpurgo, *New J. Phys.* **10**, 033031 (2008).
- [35] A. G. Zabrodskii, *Philos. Mag. B* **81**, 1131 (2001).
- [36] C. O. Yoon, M. Reghu, D. Moses, A. J. Heeger, Y. Cao, T.-A. Chen, X. Wu, and R. D. Rieke, *Synth. Met.* **75**, 229 (1995).
- [37] A. L. Efros and B. I. Shklovskii, *Electronic Properties of Doped Semiconductors* (Springer-Verlag, 1984).
- [38] S. Wang, M. Ha, M. Manno, C. Daniel Frisbie, and C. Leighton, *Nat. Commun.* **3**, 1210 (2012).
- [39] K. Shimakawa, *Phys. Rev. B* **39**, 12933 (1989).
- [40] L. R. Wienkes, C. Blackwell, T. Hutchinson, and J. Kakalios, *J. Appl. Phys.* **113**, 233707 (2013).
- [41] M. J. Panzer and C. D. Frisbie, *J. Am. Chem. Soc.* **129**, 6599 (2007).
- [42] M. Li, T. Graf, T. D. Schladt, X. Jiang, and S. S. P. Parkin, *Phys. Rev. Lett.* **109**, 196803 (2012).
- [43] E. Menard, V. Podzorov, S.-H. Shur, A. Gaur, M. E. Gershenson, J. A. Rogers, *Adv. Mater.* **16**, 2097, (2004).

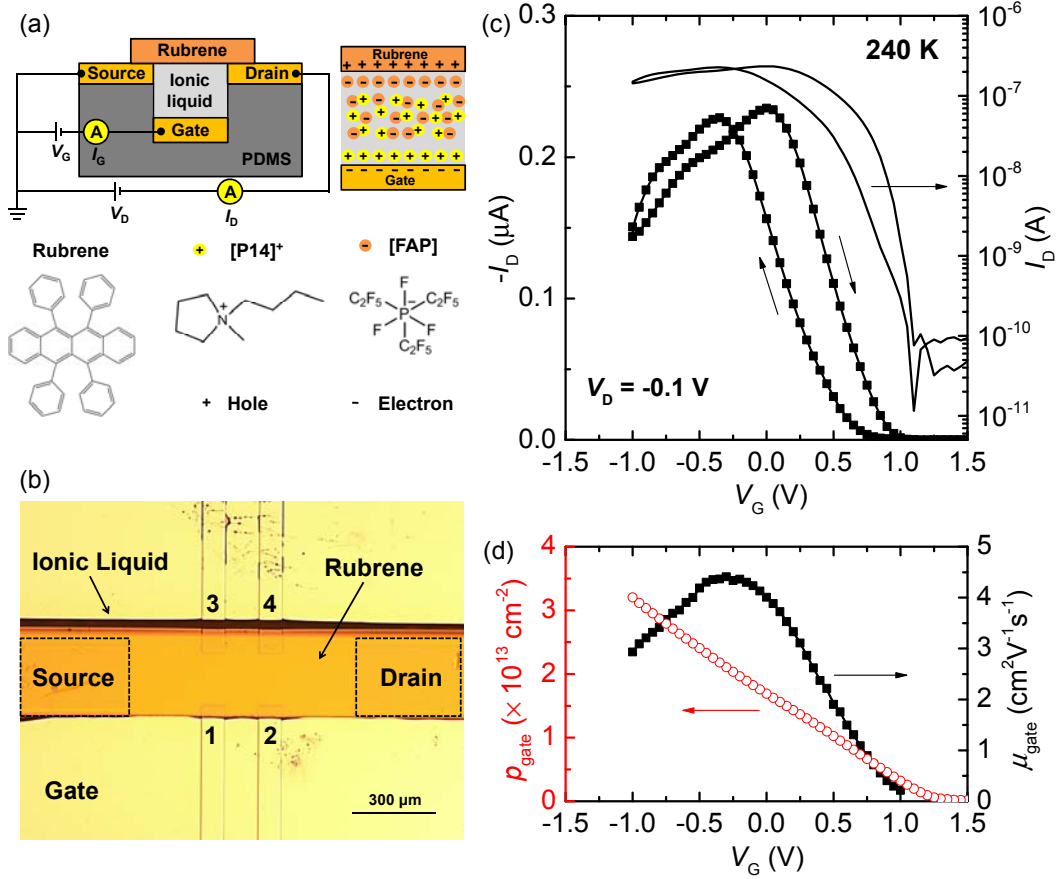


Figure 1. (a) Cross-sectional device structure with molecular structures of rubrene and [P14][FAP]. (b) Optical micrograph of a rubrene EDLT in a Hall-bar configuration. (c) Transfer characteristics of Device #1 at 240 K; sweep rate is 50 mV/s; (left axis, squares) I_D - V_G on linear-linear scale at $V_D = -0.1$ V; (right axis, lines) same I_D - V_G on log-linear scale. (d) 240 K V_G -dependent hole density p_{gate} (red, left axis) and mobility μ_{gate} (black, right axis). p_{gate} is measured from gate displacement current.

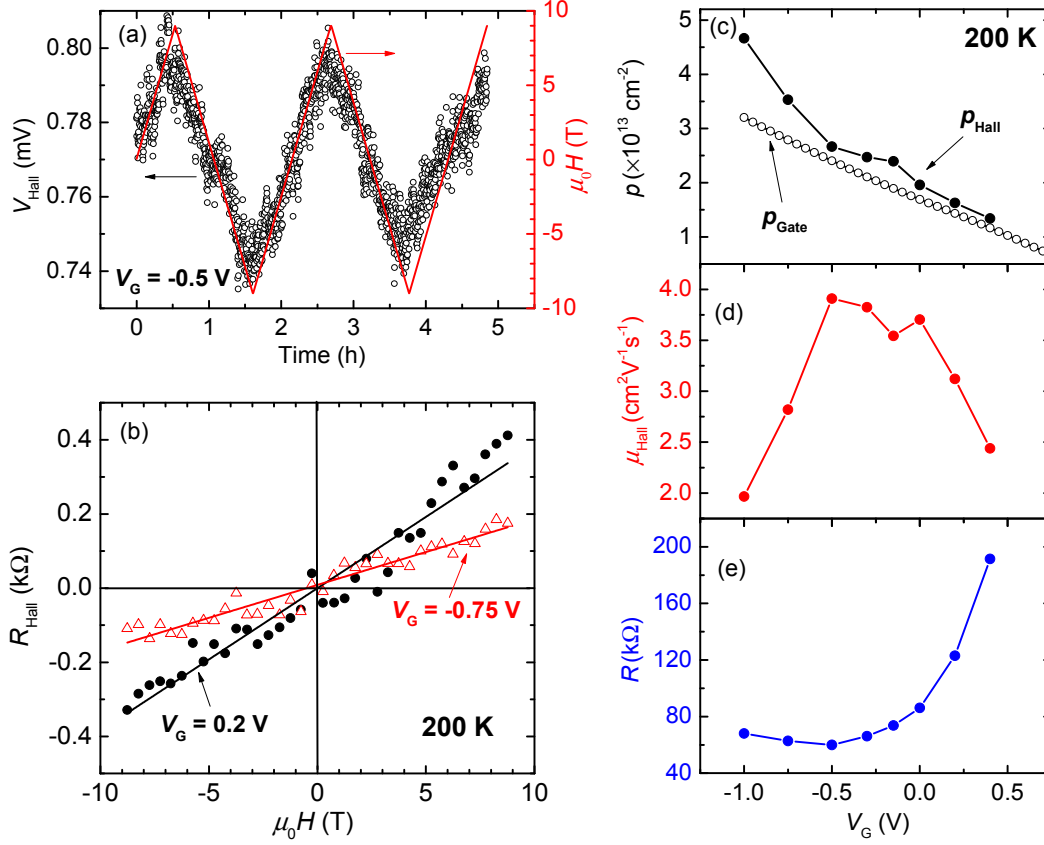


Figure 2. (a) Hall voltage (V_{Hall}) (black circles) and $\mu_0 H$ (red lines) as a function of time at $V_G = -0.5$ V and a source current of 100 nA. (b) Hall resistance (R_{Hall}) versus field ($\mu_0 H$) for $V_G = 0.2$ V (black circles) and -0.75 V (red triangles). R_{Hall} has been bin-averaged and the zero-field value has been subtracted; solid lines are linear fits. (c) Hole density measured from Hall effect (p_{Hall}) and displacement current (p_{Gate}), (d) Hall mobility (μ_{Hall}) and (e) four-terminal channel sheet resistance (R) as a function of V_G . All results are measured on Device #1.

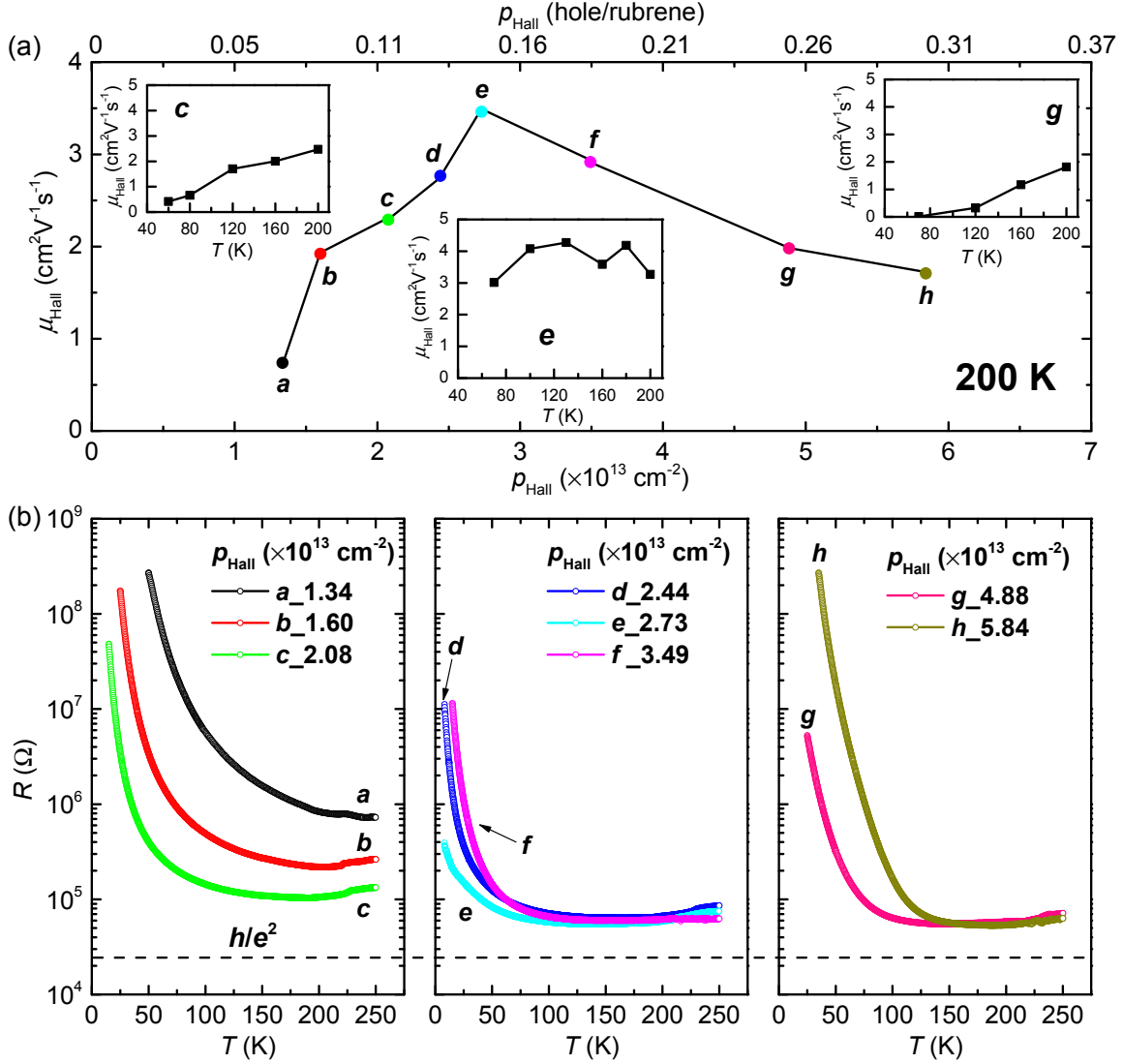


Figure 3. (a) μ_{Hall} - p_{Hall} relation in Device #2 at 200 K. Each p_{Hall} is labeled *a* through *h*. Insets: $\mu_{\text{Hall}}(T)$ before the mobility peak (*c*), at the peak (*e*) and after the peak (*g*). (b) Temperature dependence of the sheet resistance R at each p_{Hall} shown in (a).

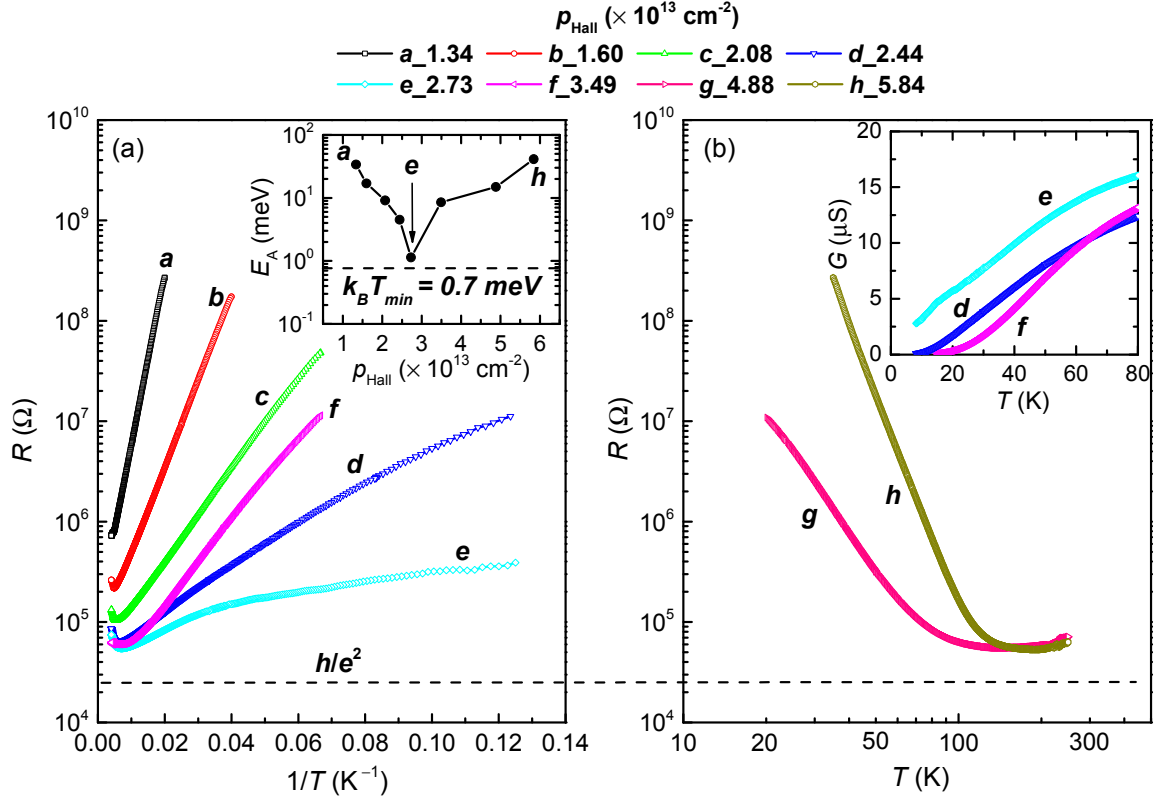


Figure 4. (a) $\log_{10}(R)$ versus T^{-1} for p_{Hall} from *a* to *f*. Inset: Low- T activation energy E_A as a function of p_{Hall} . Horizontal dashed line is $k_B T$ at the minimum temperature probed. (b) $\log_{10}(R)$ versus $\log_{10}(T)$ for p_{Hall} from *g* to *h*. Inset: Sheet conductance, G , as a function of T for *d*, *e*, and *f*.